

Analyzing the Applicability of ML Powered Microwave Sensor for UAV Based CH₄ Sensing

Vishnu S. Kumar^{1,*}, Aloy Anuja G. Mary¹, and Balasubramanian Esakki²

¹Department of Electronics and Communication Engineering, Vel Tech Rangarajan Dr. Sagunthala R&D Institute of Science and Technology, Tamil Nadu, India; Email: aloyanujamary@gmail.com (A.A.G.M.)

²Department of Mechanical Engineering, Vel Tech Rangarajan Dr. Sagunthala R&D Institute of Science and Technology, Tamil Nadu, India; Email: esak.bala@gmail.com (B.E.)

Abstract—In solid waste management, the Methane (CH₄) gas generation needs to be monitored and assessed for the environmental protection and prevent the CH₄ gas atmospheric dispersion over the dwelling regions near dump yards. Traditional methods using gas sensors measures only gas concentration at different height and never modelled or predict the gas circulation in the atmosphere. Moreover, gas circulation near every dump yard needs to be modelled based on microclimatic conditions for human safety and environmental protection. In this paper an Unmanned Aerial Vehicle (UAV) based, dispersion of CH₄ gas is monitored and assessed for the atmospheric circulation of CH₄. The CH₄ dispersion and atmospheric circulation are monitored through X-Band Bi-Static microwave transceiver sensor and Machine Learning (ML) Algorithm-Multi Linear Regression (MLR). CH₄ concentration is assessed through the RADAR's reflected signals from CH₄ gas, whereas RADAR is fixed in the UAV. The RADAR is mounted in UAV to sense concentration of CH₄ dispersion at different heights for municipal dump yard located at Thiruninravur, Tamil Nadu, India. A three-days; six-hours of field results, shows the proposed UAV-RADAR based prediction of the CH₄, performs better in the range of 250-800 ppm CH₄ concentration. The proposed UAV-RADAR system in tracing CH₄ dispersion in lower atmosphere is validated through analytical methods and modelled based on microclimatic conditions.

Index Terms—Denosing, methane detection, microwave RADAR, multi linear regression, wavelet transform, unmanned aerial vehicle

I. INTRODUCTION

In developing countries, open dumping of domestic bio-degradable solid waste is seen as common practice. Bio-degradable wastes are the major source for air pollution. The International Agency for Research on Cancer (IARC) states, air pollution as the major cause for lung cancer in human. As per the study conducted in 2019, 99% of residential communities with poor air quality area had lung related diseases [1]. AP dispersion model can be used for large scale mishap assessment. Thus, a well-designed Solid Waste Sites (SWS) and

management with an adequate monitoring and dispersion predicting system can avoid harmful air pollutants.

Gas emissions from SWS are unpredictable and leads to human hazards. At SWS, microbes convert degradable organic carbon into hydrocarbons, under anaerobic conditions. CH₄ is the major gas from SWS and has an equal impact on humans as Carbon Dioxide (CO₂) gas [2]. It is buoyant in nature and naturally ascends; experiences turbulence at atmosphere and leads to fast mixing in air. Thus, lower atmospheric environmental dispersion needs to be assessed for spread of pollutant.

Classic air quality monitoring stations provide reliable data, has low vertical coverage and never asses the discrete emission sources. Low-cost portable sensing devices are used for CH₄ dispersion measurement. Aircrafts are equipped with low-cost sensors for three-dimensional (3D) measurements based on spatial and temporal resolution, which suffers from flight-noise and altitude restrictions. Air quality monitored with tethered gas balloons mounted with low-cost sensors, evades the aircraft's height constraints but suffers from inability to do horizontal maneuvering [3]. In contrast, multi-rotor UAV is a cost-effective device for lower atmosphere and gas dispersion studies [4–9]. The recent developments in UAVs are effective in assessing the atmospheric dispersion of gas. The microwave resonator-based gas sensing also has problems such as high cost, weight and linearity.

Motivation: The microclimatic conditions [10, 11] affect the Metal-Oxide Semiconductor (MOS), electrochemical and catalytic type sensors, when used for CH₄ assessment. LiDAR based CH₄ concentration is inaccurate due to environmental light exposure.

Contribution: To solve above problems, CH₄ dispersion and concentration are measured using bi-static microwave RADAR with an operating frequency of 10.525GHz. The received RADAR signal is denoised with wavelet transform to remove the noises. The UAV is equipped with low-cost sensing system, microcontroller and ML algorithm. ML is embedded into the microcontroller and field tested over the SWS, located at Thiruninravur, Tamil Nadu, India. The results are interpolated at different altitude in the lower atmospheric range and modelled for CH₄ gas dispersion and circulation in atmosphere through GIS modelling.

Manuscript received February 10, 2023; revised March 17, 2023; accepted March 23, 2023.

*Corresponding author: Vishnu S. Kumar (email: mail2jitvishnu@gmail.com).

The organization of this article is as follow. Section II addresses the present knowledge available in the literature. Section III describes the materials and methodology employed in the study. Section IV discuss the results obtain through the experiment and the outcomes obtained from the in-situ study conducted over a municipal SWS. Finally, Section V concludes the article with summary of the work and discuss the future perspectives.

II. LITERATURE REVIEW

The gas sensing is performed in two-steps. Initially, sensing of gas is involved where the interactions between gas molecules and the sensitive material are performed. The second process is transduction, which converts the

sensing into an electronic-signal. Different types of transduction methodologies are implemented in gas sensing, such as conductometric transduction, optical transduction and electrochemical transduction. Conductometric transduction measures the redox reactions of gas molecules. In optical transduction the infrared (IR) spectral characteristics are used for gas concentration sensing. In Mass transduction, weight of gas molecules is used for gas concentration sensing and electrochemical transduction is based on the transfer of electrons. Based on the operating principle, gas sensors are classified as MOS, Catalytic, Electrochemical and IR based. Table I shows the literature survey of CH₄ gas concentration measurement using UAVs equipped with gas sensors to sense the dispersion of CH₄.

TABLE I: LITERATURE SURVEY ON DRONE ASSISTED CH₄ GAS MEASUREMENT

Ref./Year	Sensors	Methodology/algorithm for CH ₄ sensing	Advantage & disadvantage
[3] / 2017	Vertical cavity surface emitting laser, (ii) MOS and (iii) modified catalytic sensors.	UAV to monitor atmospheric gases.	MOS sensors can be utilized for direct sensing, less selective than VCSEL, which requires humidity information.
[4] / 2018	Quartz enhanced photoacoustic spectroscopy sensor.	A multi-gas sensing system based on frequencies for gas.	Physical assembly restricts the usage in an UAV.
[5] / 2019	MOS: MQ-4	CH ₄ concentration from inside a closed container with Arduino microcontroller.	Low sensitivity to mixed-gas environment.
[12] / 2020	MOS: MQ-2 & MQ-4	MQ series sensors collected CH ₄ at every 5 meters in altitude.	Authenticity of the gas selectivity needs further analysis.
[13] / 2021	Catalytic: TGS2600	A LoRa based airborne environmental monitoring system.	Communication upto 1KM without loss was showcased, but the sensor used is inclined to low concentration and are prone to chemical poisoning.
[14] / 2021	Near-infrared (NIR) off-axis integrated cavity output spectroscopy.	A NIR sensor to measure atmospheric CH ₄ .	Size reduction is required.
[15] / 2021	Electrochemical: (TGS-4161/5042), MOS: (TGS-3870/823/8100 & TGS26-00/02/03/11)	Principal component regression for CH ₄ concentration in the dry methane reforming process.	Sensor is vulnerable due to quick pressure shift, humidity and drought.
[16] / 2022	NIR absorption spectroscopy (NIR-AS)	Symmetrized dot pattern.	Sequential monitoring will be slower in multipoint analyses.
[17] / 2022	LiDAR & MQ-4	Reduced support vector machine and artificial neural network with MQ-4 sensor and LiDAR.	The LiDAR accuracy reduces due to direct sun-light exposure.

In this paper, UAV based gas sensing problems are summarized and discussed below:

- In-flight sensor performance: Accuracy of sensors that are attached to flight for gas concentration measurement depends on temperature, humidity, pressure, and direct sunlight exposure.
- Response time: The reaction time of the sensing-instrument are influenced by the flight speed, which will directly affect the overall flight endurance.
- Limit of Detection (LoD): The maxi-min limits must be focused, as datasheet values are usually measured under the controlled laboratory settings.
- Dynamic range: Based on the distance between the source and the flight, the gas-concentration varies. Thus, sensor must be equipped in a flight with support of a dynamic sensing range.

In this paper, above problems are solved through, microwave sensor based CH₄ concentration measured using UAV. ML models in geospatial is used for CH₄ gas concentration measurement.

III. MATERIALS AND METHODOLOGY

In this paper, the proposed methodology overcomes the drawbacks of existing methods such as low-sensitivity, sensor poisoning and temperature dependency of traditional gas sensors. In this study, UAV has a bi-static RADAR which senses CH₄ concentration. Moreover, UAV is equipped with NodeMCU to support Internet of Things functionality and CH₄ concentration prediction through built-in ML algorithm.

A. Materials

Atmospheric CH₄ sensing is different from level-based gas sensing. Atmospheric CH₄ gas sensing through an UAV has certain limitations with MQ-4 sensor-based measurement such as altitude, temperature, vibration of sensor and consumes high energy. In this paper, X-band HB100 bi-static RADAR with an operating frequency of 10.525GHz and coverage range of 2m to 16m is used for CH₄ sensing. Instrumentation amplifier (AD-620) is

utilised for RADAR Intermediate Frequency (IF) signal amplification. NodeMCU, a 32-bit microcontroller with an integrated 10-bit Analog to Digital Converter (ADC) resolution is used for converting IF signals into digital values. Table II shows the components used in UAV for the atmospheric gas concentration study.

TABLE II: CHARACTERISTICS OF THE DEVICES IN UAV

Parameter	Working principle	Equipment model	Range
Bi-static RADAR	Doppler effect	HB100	2m to 16m
Gas sensor	Chemi-resistance	MQ-4	200ppm to 1000ppm
Instrumentation amplifier	Amplification	AD-620	1A to 10,000 A
Microcontroller	32-bit MCU	NodeMCU-12E	10-bit ADC resolution

B. Radar IF Signal Amplification Circuit

A custom Printed Circuit Board (PCB) is designed and fabricated that integrates components as listed in Table II. Fig. 1 shows the overall circuit diagram of IF signal amplification. Instrumentation amplifier (AD620) is placed between the input of NodeMCU and the bistatic RADAR sensor. The top-view of the assembled PCB is shown in the Fig. 2.

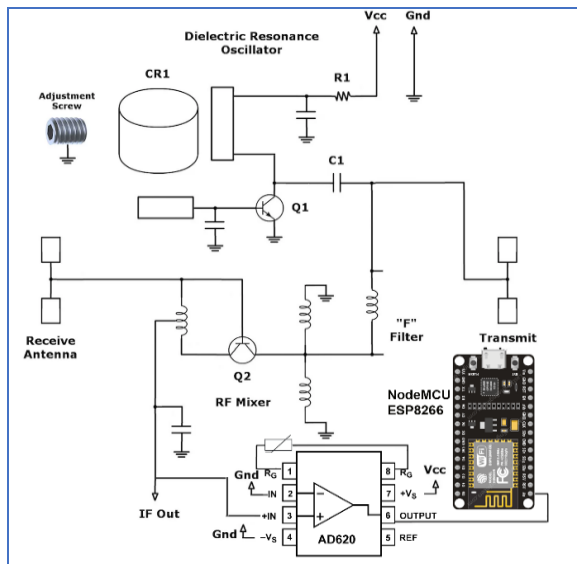


Fig. 1. CH₄-Sensing schematic diagram.

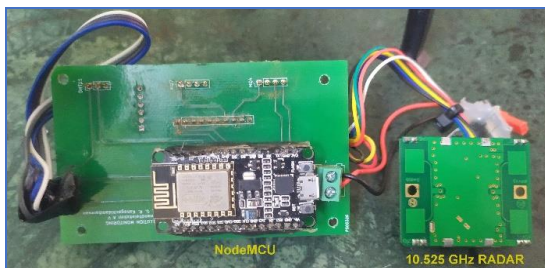


Fig. 2. CH₄ sensing-fabricated and assembled PCB.

C. Methodology

In this paper, a two-stage process have been performed. Initially sensed signals are processed with wavelet

transform and then reconstructed. Second, ML model is applied to the collected IF signal and the laboratory values of known concentrations of CH₄. The wavelet reconstructed signal amplitude is proportional to CH₄ gas concentration. In this study, a municipal SWS at Thiruninravur, Tamil Nadu, India is selected for atmospheric CH₄ concentration measurement. The IF signals of the RADAR are amplified using an instrumentation amplifier. The MLR algorithm is chosen due to its low memory consumption in NodeMCU. The embedded MLR algorithm predicts the CH₄ concentration value from the denoised signal, considering the micro-climatic conditions. The predicated values are transferred to Google Sheet using Hyper Text Transfer Protocol (HTTP) as shown in Fig. 3. The collect values from ML model are used for interpolation of the dispersion of gas in the atmospheric region and model the atmospheric air circulation. Fig. 4 illustrates the overall flow of the study.

	A	B	C	D	E	F	G
	Date	Time	temperature	humidity	Altitude	CO volt	CH4 volt
2	2022/10/02	11:50:29 AM	29.6	94	3	2.649	0.00234
3	2022/10/02	11:50:06 AM	29.5	93	2.6	2.646	0.002331
4	2022/10/02	11:49:44 AM	29.6	93	2.2	2.643	0.002313
5	2022/10/02	11:49:22 AM	29.6	93	2	2.637	0.002292
6	2022/10/02	11:48:57 AM	29.3	93	2	2.631	0.002277
7	2022/10/02	11:48:25 AM	30.5	88	1.9	2.628	0.002262
8	2022/10/02	11:48:02 AM	30.8	87	1.5	2.628	0.002262
9	2022/10/02	11:47:40 AM	31.3	87	1.3	2.619	0.002238
10	2022/10/02	11:47:18 AM	31.2	89	1	2.628	0.002247
11	2022/10/02	11:46:56 AM	30.7	88	1	2.619	0.002217
12	2022/10/02	11:46:34 AM	31.1	86	2	2.61	0.002217
13	2022/10/02	11:46:12 AM	31.2	84	2.5	2.598	0.002202
14	2022/10/02	11:45:53 AM	32.1	79	2.6	2.577	0.002154
15	2022/10/02	11:45:33 AM	32.9	77	3.3	2.574	0.002148
16	2022/10/02	11:45:09 AM	33.7	74	3.5	2.577	0.002157
17	2022/10/02	11:44:55 AM	34.8	69	4	2.571	0.002145
18	2022/10/02	11:44:33 AM	34.6	72	7.5	2.586	0.002154
19	2022/10/02	11:44:13 AM	34.5	72	6.9	2.577	0.002151
20	2022/10/02	11:43:55 AM	34.7	68	6.4	2.571	0.002148
21	2022/10/02	11:43:32 AM	34.8	68	6	2.583	0.002154
22	2022/10/02	11:43:20 AM	35.5	67	4.7	2.589	0.002157
23	2022/10/02	11:42:58 AM	35.5	67	4.2	2.598	0.002175
24	2022/10/02	11:42:35 AM	35.9	65	3.5	2.601	0.002187
25	2022/10/02	11:42:13 AM	36.3	65	3	2.628	0.002235

Fig. 3. Screenshot of the data collected in Google sheet.

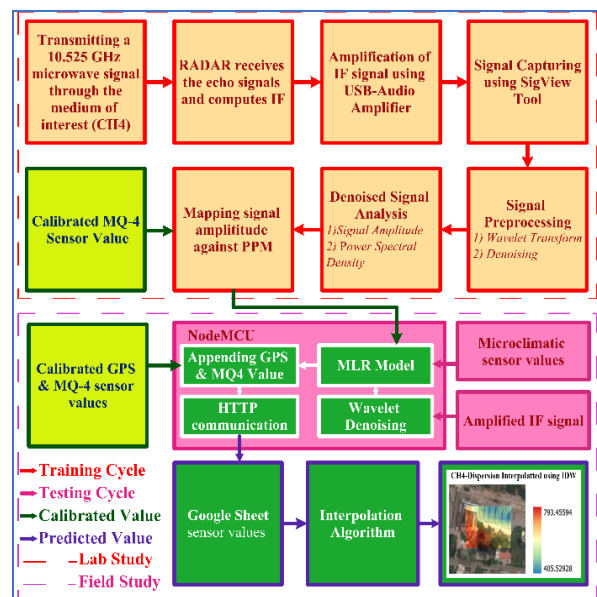


Fig. 4. The overall block diagram for predicting CH₄ dispersion & gas circulation at atmospheric level.

D. Microwave Energy Transfer Process in CH₄ at Atmospheric Level

Microwave signals, interact with matter such as solid, liquid and gas at the level of individual atoms, electrons, and magnetic dipoles. Microwave-matter interaction depend on medium's reflection, absorption or scattering of the wave, the amplitude and frequency variations in the received signal are used for sensing the medium. In CH₄ sensing, electromagnetic radiation from the RADAR are absorbed and reflected. RADAR equation relates the reflectivity, transmitted power, antenna aperture and conductivity of the medium. The reflectivity and transmittance are calculated with the general power density equation (P_d) in W/m² as

$$P_d = \frac{P_t G_t}{4\pi R^2} \quad (1)$$

where P_t represents power of the transmitter antenna, G_t represents gain of the transmitter antenna and R represents the distance between RADAR and CH₄ plume.

The power of the received signal, P_r in W/m², at the receiver antenna in the absence of CH₄ medium is calculated using Eq. (2):

$$P_r = P_d A_e = \left(\frac{P_t G_t}{4\pi R^2} \right) \left(\frac{\lambda^2 G_r}{4\pi} \right) \quad (2)$$

where G_r is the gain of receiver antenna and λ is the RADAR signal wavelength, and $A_e = (\lambda^2 G_r)/(4\pi)$ is the antenna aperture in m².

To calculate the power of received signal (P_{rt}) under the presence of CH₄, power at receiver is calculated as the power of the reflected signal from CH₄ plume minus free space attenuation, i.e., Eq. (2) is modified as per the Maxwell's equation and includes the conductivity of the medium as

$$P_{rt} = \frac{P_t G_t \sigma}{4\pi R^2} \text{ W/m}^2 \quad (3)$$

where σ represents the conductivity of the medium. CH₄ is considered as lossy dielectric ($\sigma \neq 0$) molecule.

The four covalent bonds exist between the central carbon and all four hydrogen atoms; no free electrons in the molecule. Lossy medium has a wave dispersion, which is characterized based on the complex dielectric constant denoted by $\epsilon = (\epsilon' - j\epsilon'')$; where ϵ' is the relative permittivity, responsible for reflection and imaginary part, ϵ'' the loss factor responsible for absorption. As microwaves target rotational modes in CH₄ gas-molecules, the intrinsic impedance of the microwave is calculated using Eq. (4).

$$\eta = \sqrt{\frac{j\omega\mu}{\sigma + j\omega\epsilon}} = \sqrt{\frac{\mu}{\epsilon}} \left(1 - j \frac{\sigma}{\omega\epsilon} \right)^{-1/2} \quad (4)$$

where j is the imaginary unit, ω is the angular frequency of the electromagnetic wave and μ is the magnetic permeability of the medium.

Dielectric materials will have some conductivity $\sigma \ll \omega\epsilon$, where the term $\sigma/\omega\epsilon$ is referred as the loss tangent as defined in Eq. (5).

$$\tan \theta = \frac{\sigma}{\omega\epsilon} \quad (5)$$

Due to lower conductivity, the electric and magnetic fields in the medium are no-longer in phase. Thus, Eqs. (6) and (7) represent the Maxwell's frequency domain solution, the propagation constant γ is derived in Eq. (8):

$$\nabla^2 \mathbf{E} = j\omega\mu(\sigma + j\omega\epsilon)\mathbf{E} \quad (6)$$

where \mathbf{E} represents the electric field.

$$\nabla^2 \mathbf{H} = j\omega\mu(\sigma + j\omega\epsilon)\mathbf{H} \quad (7)$$

where \mathbf{H} represents the magnetic field.

$$\gamma = \sqrt{j\omega\mu(\sigma + j\omega\epsilon)} = \alpha + j\beta \quad (8)$$

where α represents the attenuation constant and β represents the phase constant.

In RADAR based gas sensing, orientation of electric fields polarization plays a vital role. CH₄ is a non-polar molecule, but still exhibits a dipole moment in ground vibronic state, because of its tetrahedral spherical top structure, whose conductivity is not to be neglected [18]. Angle between UAV and the RADAR's trans-receiver antenna is perpendicular in nature, polarization happens in vertical-vertical mode; whose reflectivity and transmittance are calculated as

$$\Gamma_c = \frac{(\epsilon_r - jx)\sin\psi - \sqrt{(\epsilon_r - jx) - \cos^2\psi}}{(\epsilon_r - jx)\sin\psi + \sqrt{(\epsilon_r - jx) - \cos^2\psi}} \quad (9)$$

$$T_v = \frac{2\sqrt{(\epsilon_r - jx) - \cos^2\psi}}{\sqrt{(\epsilon_r - jx) - \cos^2\psi} + (\epsilon_r - jx)\sin\psi} \quad (10)$$

where Ψ represents angle of incidents, $\epsilon_r = \epsilon/\epsilon_o$ is the relative permittivity, $x = 18\sigma/f_{\text{GHz}}$ and $\psi = 90^\circ - \theta_i$ defined as pseudo-Brewster angle.

E. CH₄ Concentration Evaluation Using Radar System at Laboratory Level-A Prototype Model

Laboratory scale CH₄ was produced from waste coal washery rejects available at the institute's bio-gas pilot-plant [19], whose concentration was assessed using Geotech Bio-gas analyzer (BIOGAS5000). Fig. 5 (next page) shows the laboratory level CH₄ production from the coal waste, which is later transferred to a circular butyl rubber tube. An open-close knob was fixed in the rubber tube and to model the SWS CH₄ dispersion. The RADAR's IF signals were acquired with Universal Serial Bus (USB) Data Acquisition System (DAQ). The captured signals were denoised using MATLAB wavelet toolbox to get discrete values as shown in Table III, which is later used to design a ML model. The concentration of CH₄ was simultaneously measured using pre-calibrated MQ-4 sensor and the bistatic-RADAR as shown in Fig. 6.


 Fig. 5. CH₄ produced at laboratory scale.


Fig. 6. View of laboratory dataset collection.

 TABLE III: LABORATORY OBSERVATION: SIGNAL AMPLITUDE VS RELATIVE CH₄ CONCENTRATION

Distance (m)	Wind speed (m/s)	Observed amplitude (mV)	Atmospheric temperature (°C)	Humidity (%)	Average CH ₄ concentration (ppm)
0.3	2	475-500	25.23	72.34	877.06
0.3	3	450-475	27.05	78.30	815.13
0.3	4	425-450	28.97	65.92	765.47
0.3	5	400-425	31.20	65.92	715.05
0.6	2	335-365	25.23	72.34	638.50
0.6	3	300-335	27.05	78.30	612.13
0.6	4	275-300	28.97	65.92	585.17
0.6	5	250-275	31.20	65.92	560.12
1.0	2	275-200	25.23	72.34	505.16
1.0	3	265-275	27.05	78.30	487.87
1.0	4	225-265	28.97	65.92	375.09
1.0	5	200-225	31.20	65.92	288.33

F. UAV Based Dispersion Measurement

The low-cost drone is assembled using carbon-fibre frame (S500). Holybro-Pixhawk4 is selected as the controlling platform and controls the four 960 kV BLDC-motors. The UAV is equipped with 5200 mAh LiPo battery and supports 20-minute flight endurance. The configuration view of the assembled UAV is shown in the Fig. 7. The UAV is made to fly over SWS. The IF signal, after interaction with CH₄ value is used for prediction of CH₄ concentration after processing with wavelet transform. Using CH₄ concentration values obtained from UAV, Geographic Information System (GIS) tool is used for atmospheric dispersion and circulation of CH₄ gas modelling.

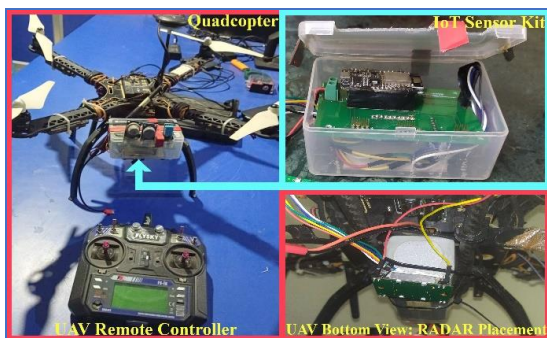


Fig. 7. Configuration of the UAV platform.

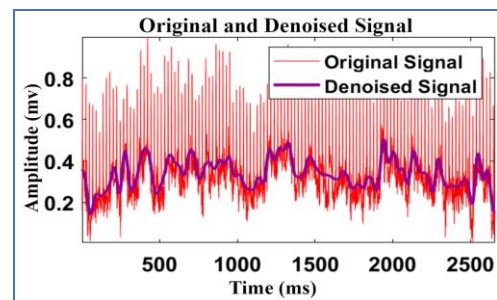
IV. RESULTS

In this paper, a microwave RADAR is used for real-time gas monitoring by measuring the IF signal amplitude. This allows us to monitor the CH₄ concentration without the drawbacks mentioned in the literature section. The system allows estimating the dispersion of the CH₄ being evaluated by fusing, microclimatic-conditions, Global Positioning System (GPS) value and the data from the RADAR, where time is the common attribute.

A. Wavelet Denoising of IF Signals from Radar

Interference from multiple sources like propeller and reflected-signals from other sources causes noise in RADAR signal. To denoise the sensed signal, wavelet transformation is used. After filtering, prediction of CH₄ accuracy is improved [20, 21]. The RADAR signals are generally characterized as non-periodic signals with rapid transients, analysis using conventional Fourier analysis is challenging. Thus, wavelet transform has been utilized, which separates the noise from the signal by separating the raw-signal into its low and high frequency components. The coefficients of the noise signals are discarded through threshold processing, and an inverse transform is performed on the remaining transform coefficients to reconstruct the original-signal. MATLAB-Wavelet analyzer and denoiser toolsets are utilized for both low frequency approximation output (A) and high frequency details (D) measurement. Inspired from the [22] author's work, Coiflet (Coif) wavelet transform was used in this study. A case-to-case analyses has been conducted using Coif wavelet with subclasses one to five and approximation/detail levels ranging from one to five as illustrated in Fig. 9 (next page).

The Peak Signal-To-Noise Ratio (PSNR), Structural Similarity Index Measure (SSIM) and Correlation are used as performance metric to choose the right wavelet denoising process. The statistical mean, median and standard deviation of the denoised signal is obtained, on using different subclass and A-level. Based on the analyses, subclass-five with A-level five denoises IF signal better than other subclass and A-level. "Fixed form threshold" is chosen as the thresholding method with "Non-White noise" as the denoise structure. Fig. 8 shows the denoised signal in the acquired under laboratory conditions. The controlled release of CH₄ was performed and emulated the SWS emission-dispersion scenario under atmospheric pressure, temperature and wind speed.


 Fig. 8. Comparison between denoised signal and raw-signal in the presence of CH₄.

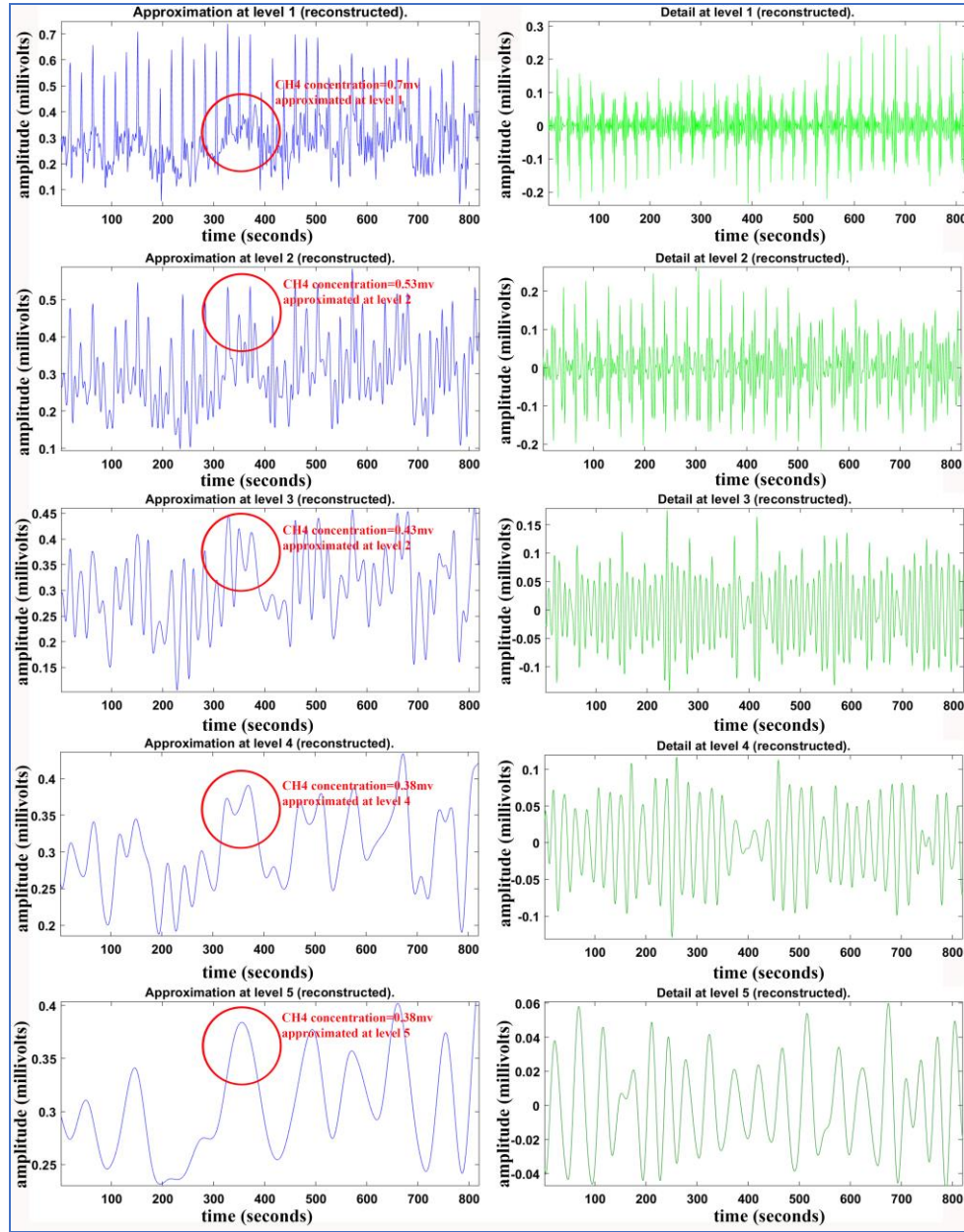


Fig. 9. Coif5 transform analysis of the low and high frequency components of the IF signal at levels 1 to 5.

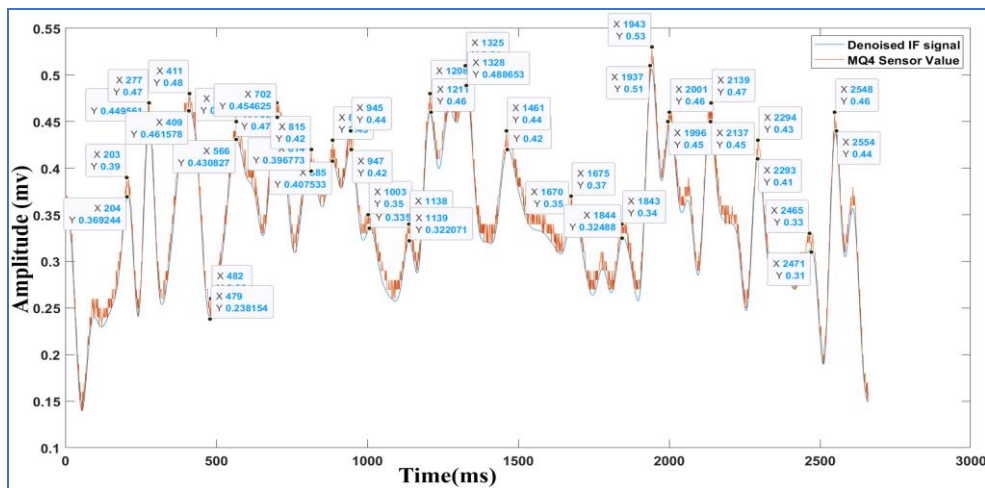


Fig. 10. Denoised IF signal's amplitude vs time plot.

The bi-static RADAR and a pre-calibrated MQ-4 sensor are used to sense the CH₄ plume simultaneously. The RADAR sensed signal is denoised and reconstructed as in Fig. 10 (previous page), which projects the denoised signal read by RADAR at 30 cm distance from CH₄ emission point. The amplitude of the signal is noted against the known CH₄ concentration.

B. MLR Model for Atmospheric CH₄ Dispersion Modelling

The MLR models establishes relationship between dependent and independent variables as defined as $y = \beta_0 + \sum_{i=1}^n \beta_i x_i$, where β represents regression coefficients, x represents the set of independent variables, n represents the number of independent variables and y represents the dependent variable. In this study, the distance between source and UAV, temperature, humidity and IF-signal amplitude are used as independent variables. The regression between the dependent and independent variables are inspired based on the [23] author's work. A hundred and fifty-seven sample points were used to train the model. The statistical values and variance analysis of the proposed MLR model are tabulated in Table IV and Table V respectively. The ESP8266 based NodeMCU microcontroller with a 64KB of RAM is used for implementation of wavelet-denoising, MLR and HTTP. Equation (11) shows the CH₄ prediction algorithm.

$$\text{CH}_4 = 1139.31 - (440.33\text{WS}) - (13.02D) + (0.33A) - (14.3T_A) + (1.11H) \quad (11)$$

where H represents humidity, T_A represents atmospheric temperature, A represents RADAR's IF signal amplitude, D represents distance between RADAR and CH₄ plume, and WS represents wind speed.

TABLE IV: MLR MODEL: STATISTICS

Predictor	Coefficient	Estimate	Standard Error	t -statistic	p -value
Constant	β_0	1139.31	2442.65	0.47	0.66
WS	β_1	-440.33	120.02	-3.67	0.01
D	β_2	-13.02	218.03	-0.06	0.95
A	β_3	0.33	0.39	0.86	0.43
T_A	β_4	-14.3	111.02	-0.13	0.9
H	β_5	1.11	3.11	0.36	0.73

TABLE V: MLR MODEL-ANALYSES OF VARIANCE

Source	Degrees of freedom	Regression standard error	Mean squared errors	F -statistic	p -value
Regression	5	326997.4	65399.47	42.01	0
Residual error	6	9340.39	1556.73	-	-
Total	11	336337.8	30576.16	-	-

C. GIS Based CH₄ Gas Circulation Modelling

The accurate measurement of AQ data is of high demand, particularly three-dimensional (3D) mapping and visualization of AQ is an efficient choice to understand the dispersion of pollutants in the air. Present field study focuses on collecting CH₄ dispersion over a municipal SWS. The test was conducted over a dump-yard located at latitude 13°8'10.4928" N and longitude

80°2'59.1036" E. The aerial view captured of the study-field, from an UAV is shown in Fig. 11.

The experiment is conducted over the dump yard for the purpose of studying the 3D distribution of the CH₄. The acquisition of CH₄ concentration was performed on 29th September 2022, 2nd October 2022 and on 4th October 2022 with an average wind-speed 3 m/s to 4 m/s. Fig. 12 shows flight path of the UAV over the SWS on different days. For first two days, the drone was flown in manual mode and examined the stability, maneuverability, power consumption and the communication between onboard-IoT module and Google Sheet. UAV had a vertical ascend and descent between 2 m to 7 m Above the Ground Level (AGL) as shown in Fig. 13.



Fig. 11. Isometric view of the test-site.



Fig. 12. Flight paths of the field testing.



Fig. 13. UAV hovering over different sections.

The drone was flown in an automatic mode on day three, based on the field experience gathered. UAV was programmed to hover 10 seconds between every one meter and a vertical flight between the ranges of 2m to 6m and collected the atmospheric CH₄ dispersion data. The measured values are plotted against the altitude and obtain CH₄ dispersion based on spatial and temporal regions. The vertical profile represents the average values based on the Inverse Distance Weighted (IDW) technique as in Figs. 14.-17 shows the comparison between CH₄

concentration at different heights of same the latitude-longitude pair, over a municipal dump yard at 4 m, 5 m and 6 m AGL.

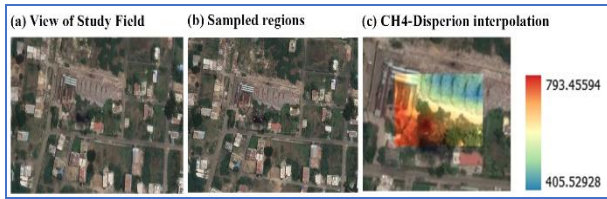


Fig. 14. CH₄ dispersion plotted using IDW.

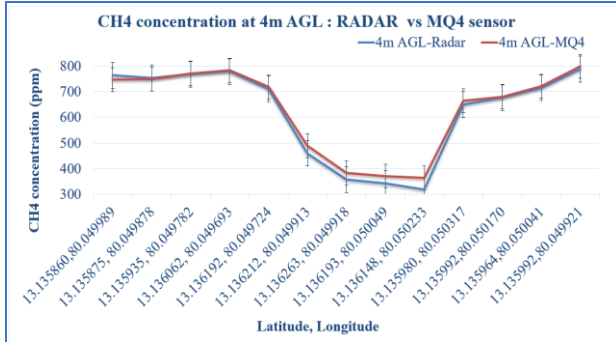


Fig. 15. Comparison between predicted vs MQ-4 readings at 4m AGL.

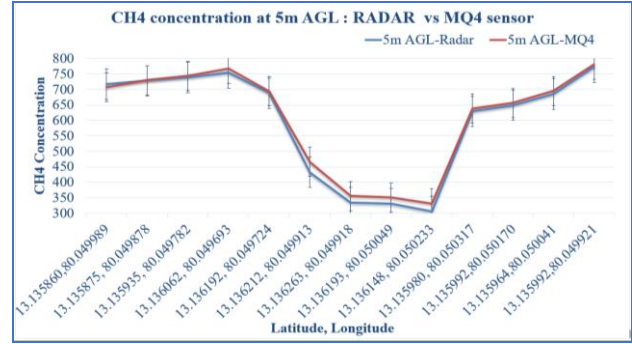


Fig. 16. Comparison between predicted vs MQ-4 readings at 5m AGL.

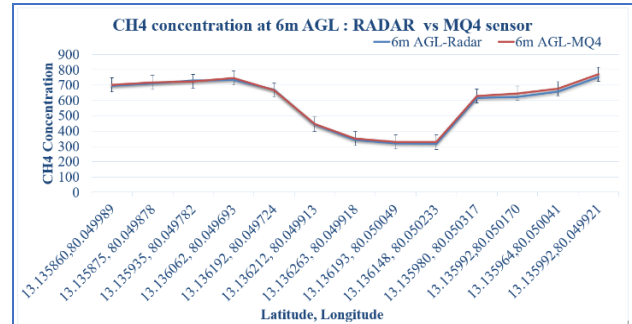


Fig. 17. Comparison between predicted vs MQ-4 readings at 6m AGL.

TABLE VI: COMPARISON WITH OTHER REPORTED WORKS

Ref./Year	Sensor type	Algorithm used		Performance metric		
		Algorithm name	Scope to be embedded in MCU	IoT enabled	UAV mounting feasibility	Results obtained
[24] / 2021	Electrochemical	Artificial neural networks	No	No	No	Accuracy>98%
[25] / 2021	Direct absorption spectroscopy	Deep neural networks	No	No	No	$R^2=0.98$
[26] / 2021	Tin-oxide	Artificial neural network	No	No	Yes	RMSE 0.2 ppm
[27] / 2022	Near-infrared laser	Linear regression	Yes	No	No	fitting degree >99.97%
[28] / 2022	Interband cascade LASER	Partial least squares regression	No	No	No	$R^2=0.99$
[17] / 2022	LiDAR	ANN	No	No	Yes	$R^2=0.99$
This Paper	Bi-static microwave radar	MLR	Yes	Yes	Yes	$R^2=0.97$

D. Comparison between Traditional Methods and RADAR Method

The proposed microwave-based sensing system produced better results in terms of CH₄ mapping. The RADAR sensor is free from ambient light, humidity and temperature turbulence. Table VI compares the proposed work with traditional methods of CH₄ sensing.

V. CONCLUSION

Monitoring CH₄ dispersion and atmospheric circulation plays a vital role in reducing air pollution and for human safety through removing solid waste regions with high-concentration. A cost-effective CH₄ dispersion assessment is presented in this paper. The proposed method involves mounting an X-band bistatic microwave RADAR beneath a small UAV to measure CH₄ dispersion at dynamic heights and locations. CH₄ concentration with respect to IF signal amplitude and microclimatic conditions is computed. The data recorded

is transmitted to cloud and then dispersion modelling is performed. The CH₄ concentration is in the range of 250 ppm to 800 ppm which coincides with the measurements of a typical landfill. The UAV based test flights identified variations in gas-sensing over low-concentration areas. Our next task is to incorporate additional sensors such as infrared cameras to identify the relation between terrains and CH₄ emission. This study utilized a unique way to combine the advantages of sensor, signal analysis and ML for monitoring CH₄ concentration during both day and night time.

CONFLICT OF INTEREST

The authors declare no conflict of interest.

AUTHOR CONTRIBUTIONS

V. S. Kumar formulated and introduced the concept while A. A. G. Mary took on the responsibility of overseeing the project's direction and organization. V. S.

Kumar conducted the experiment and created the theory in collaboration with B. Esakki. A. A. G. Mary verified the analytical methods, stimulated the inquiry, and supervised the findings. V. S. Kumar and B. Esakki participated in the field experiment and the interpretation of the findings. A. A. G. Mary and B. Esakki offered crucial feedback that aided in shaping the research, analysis, and manuscript, while V. S. Kumar wrote the manuscript. All authors collectively deliberated the outcomes and contributed to the final version of the manuscript.

REFERENCES

- [1] H. Ouyang, X. Tang, R. Kumar, *et al.*, "Toward better and healthier air quality: Implementation of WHO 2021 global air quality guidelines in Asia," *Bull. Am. Meteorol. Soc.*, vol. 103, no. 7, pp. E1696-E1703, Jul. 2022.
- [2] P. Guzmán, P. T. Carrasco, M. M. S. Varel, *et al.*, "Effects of air pollution on dementia over Europe for present and future climate change scenarios," *Environ. Res.*, vol. 204, #112012, 2022, doi: 10.1016/J.ENVIRES.2021.112012
- [3] T. J. Schuyler and M. I. Guzman, "Unmanned aerial systems for monitoring trace tropospheric gases," *Atmosphere*, vol. 8, no. 10, 2017, doi:10.3390/ATMOS8100206
- [4] Q. Zhang, J. Chang, Z. Cong, *et al.*, "QEPAS sensor for simultaneous measurements of H₂O, CH₄, and C₂H₂ using different QTFs," *IEEE Photonics J.*, vol. 10, no. 6, 2018, doi:10.1109/JPHOT.2018.2880187
- [5] S. Yang, Y. Liu, N. Wu, *et al.*, "Low-cost, Arduino-based, portable device for measurement of methane composition in biogas," *Renew. Energy*, vol. 138, pp. 224-229, Aug. 2019, doi: 10.1016/J.RENENE.2019.01.083
- [6] R. Sharma and R. Arya, "UAV based long range environment monitoring system with industry 5.0 perspectives for smart city infrastructure," *Comput. Ind. Eng.*, vol. 168, #108066, Jun. 2022, doi: 10.1016/J.CIE.2022.108066
- [7] A. Cozma, A. C. Firculescu, D. Tudose, *et al.*, "Autonomous multi-rotor aerial platform for air pollution monitoring," *Sensors (Basel)*, vol. 22, no. 3, 2022, doi:10.3390/s22030860
- [8] S. Duangsuwan, P. Prapruetdee, M. Subongkod, *et al.*, "3D AQI mapping data assessment of low-altitude drone real-time air pollution monitoring," *Drones*, vol. 6, no. 8, 2022, doi:10.3390/DRONES6080191
- [9] G. Allen, P. Hollingsworth, K. Kabbabe, *et al.*, "The development and trial of an unmanned aerial system for the measurement of methane flux from landfill and greenhouse gas emission hotspots," *Waste Manag.*, vol. 87, pp. 883-892, Mar. 2019, doi: 10.1016/J.WASMAN.2017.12.024
- [10] A. N. Abdullah, K. Kamarudin, L. M. Kamarudin, *et al.*, "Correction model for metal oxide sensor drift caused by ambient temperature and humidity," *Sensors (Basel)*, vol. 22, no. 9, 2022, doi:10.3390/s22093301.
- [11] A. N. Abdullah, K. Kamarudin, S. M. Mamduh, *et al.*, "Effect of environmental temperature and humidity on different metal oxide gas sensors at various gas concentration levels," in *Proc. IOP Conf. Ser.: Mater. Sci. Eng.*, vol. 864, no. 1, #012152, May 2020, doi:10.1088/1757-899X/864/1/012152
- [12] S. Pochwała, A. Gardecki, P. Lewandowski, *et al.*, "Developing of low-cost air pollution sensor-measurements with the unmanned aerial vehicles in Poland," *Sensors (Basel)*, vol. 20, no. 12, 2020, doi:10.3390/s20123582
- [13] S. Liu, X. Yang, and X. Zhou, "Development of a low-cost UAV-based system for CH₄ monitoring over oil fields," *Environ. Technol.*, vol. 42, no. 20, pp. 3154-3163, 2021.
- [14] K. Zheng, C. Zheng, H. Zhang, *et al.*, "Near-infrared off-axis integrated cavity output spectroscopic gas sensor for real-time, in situ atmospheric methane monitoring," *IEEE Sensors J.*, vol. 21, no. 5, pp. 6830-6838, Mar. 2021.
- [15] D. Dobrzyniewski, B. Szulczyński, T. Dymerski, *et al.*, "Development of gas sensor array for methane reforming process monitoring," *Sensors (Basel)*, vol. 21, no. 15, 2021, doi:10.3390/s21154983
- [16] W. Ye, X. Xu, Z. Xia, *et al.*, "Graphical characterization of infrared absorption spectroscopic gas sensor using symmetrized dot pattern," *Infrared Phys. Technol.*, vol. 123, #104152, Jun. 2022, doi: 10.1016/J.INFRARED.2022.104152
- [17] S. K. Sonka, P. Kumar, R. C. George, *et al.*, "Detection and estimation of natural gas leakage using UAV by machine learning algorithms," *IEEE Sensors J.*, vol. 22, no. 8, pp. 8041-8049, Apr. 2022.
- [18] C. W. Holt, *The Microwave Rotational Spectrum of Methane in the Ground Vibronic State*, University of British Columbia Library, 1976, doi: 10.14288/1.0061029
- [19] V. Ponnudurai, R. Rajarathinam, K. S. Muthuvelu, *et al.*, "Investigation on the utilization of coal washery rejects by different microbial sources for biogenic methane production," *Chemosphere*, vol. 287, no. 2, #132165, Jan. 2022, doi: 10.1016/J.CHEMOSPHERE.2021.132165
- [20] L. Chien, Y. Wang, A. Shi, *et al.*, "Wavelet filtering algorithm for improved detection of a methane gas sensor based on non-dispersive infrared technology" *Infrared Phys. Technol.*, vol. 99, pp. 284-291, Jun. 2019.
- [21] J. Ji, Y. Huang, M. Pi, *et al.*, "Performance improvement of on-chip mid-infrared waveguide methane sensor using wavelet denoising and Savitzky-Golay filtering," *Infrared Phys. Technol.*, vol. 127, #104469, Dec. 2022.
- [22] W. Ye, X. Xu, C. Peng, *et al.*, "A LabVIEW -based TDLAS methane detection system using a wavelet denoising method," *Micro. & Optical Tech. Letters*, 2021, doi:10.1002/MOP.33076
- [23] E. Rossi, I. Pecorini, and R. Iannelli, "Multilinear regression model for biogas production prediction from dry anaerobic digestion of OFMSW," *Sustainability*, vol. 14, no. 8, #4393, 2022, doi:10.3390/SU14084393
- [24] S. Halley, L. Tsui, and F. Garzon, *et al.*, "Combined mixed potential electrochemical sensors and artificial neural networks for the quantification and identification of methane in natural gas emissions monitoring," *J. Electrochem. Soc.*, vol. 168, no. 9, #097506, Sept. 2021, doi:10.1149/1945-7111/AC2465
- [25] L. Tian, J. Sun, J. Chang, *et al.*, "Retrieval of gas concentrations in optical spectroscopy with deep learning," *Measurement*, vol. 182, #109739, Sept. 2021.
- [26] R. R. Martinez, D. Santaren, O. Laurent, *et al.*, "The potential of low-cost tin-oxide sensors combined with machine learning for estimating atmospheric CH₄ variations around background concentration," *Atmosphere*, vol. 12, no. 1, #107, 2021, doi:10.3390/ATMOS12010107
- [27] Z. Xi, K. Zheng, C. Zheng, *et al.*, "Near-infrared dual-gas sensor system for methane and ethane detection using a compact multipass cell," *Front. Phys.*, vol. 10, #107, Mar. 2022, doi:10.3389/fphy.2022.843171
- [28] G. Menduni, A. Zifarelli, A. Sampaolo, *et al.*, "High-concentration methane and ethane QEPAS detection employing partial least squares regression to filter out energy relaxation dependence on gas matrix composition," *Photoacoustics*, vol. 26, #100349, Jun. 2022, doi: 10.1016/J.PACS.2022.100349

Copyright © 2023 by the authors. This is an open access article distributed under the Creative Commons Attribution License (CC BY-NC-ND 4.0), which permits use, distribution and reproduction in any medium, provided that the article is properly cited, the use is non-commercial and no modifications or adaptations are made.



Vishnu S. Kumar received Master degree in Engineering (M.E., VLSI Design) and Business Administration (M.B.A., Technology Management) at Anna University, Chennai, India. He has two-year industrial experience as IoT engineer and 5.7 years of teaching experience. He has published three scientific papers in international journals and two research papers in conference, which also includes an IEEE conference. During his stint as assistant professor, he has received various

industrial consultancy projects. His research area includes Internet of Things, Microwave and Embedded System Design.



Aloy Anuja G. Mary received her Ph.D. degree in the field of Quantum Cryptography at College of Engineering, Guindy, Chennai, India. She has 17 years of teaching and research experience. She has presented number of papers in International Journals and International Conferences. Her main area of interest includes Internet of Things, Wireless Networks and Quantum Computing.



Balasubramanian Esakki received his Ph.D. in the field of Robotics and Control at Concordia University, Montreal, Canada. He has published two books, more than 100 Journals and Conference papers, 2 patents granted and 5 patents in the verge of grant. He received grants from various Government of India funding programs supported through DST, DRDO, ISRO, DBT. He has collaborated with Taiwan scientists under Indo-Taiwan schema (2013-16) for the

development of micro aerial flapping wing vehicles and formation control through image processing techniques. He has also collaborated with Canadian scientists in developing and deployment of UAVs for railway bridge inspection. He developed amphibious UAV for collection of water samples in remote water bodies under Indo-Korea research schemes funded by DST, Govt. of India. His research interests are UAVs, robotics, control and sensors with online data acquisition systems.